Bullseye: a leakproof search strategy for space domain awareness

Daniel Mulligan* and **Michelle Stephens**
Science Applications International Corporation

ABSTRACT

Space objects with poor position estimates are particularly important to observe, especially if they experience unpredictable perturbations or perform maneuvers. If an object's position uncertainty grows larger than a sensor's field of view (FOV), a search pattern is likely necessary to find the object. Search patterns are often simple rasters, spirals, or fences designed to cover a defined area of space. However, even if the object is within the searched area, these patterns don't guarantee an opportunity for detection. A leakproof search pattern is a sequence of sensor boresight vectors that kinematically guarantees a chance to detect an object within its searched area. We present a new leakproof search pattern, the bullseye, consisting of overlapping concentric rings of discrete dwells. A bullseye search pattern solution must meet a set of five constraints in order to guarantee that it is leakproof. They are parameterized in terms of the object's maximum angular rate across the sensor's field of regard (FOR), along with the sensor's slew capability, dwell duration, and FOV. We arrive at the leakproof constraints through kinematic arguments, and prescribe a method for determining solutions that expand the search's leakproof area with each successive ring. The solution space is complex. We discuss how the solutions change with design parameters, particularly the integration time and maximum angular rate of the object, and comment on potential optimization strategies. Finally, we examine a ratio involving the object's maximum angular rate and the sensor's FOV, dwell time, and slewing capability, and show that there is a "point of futility" – bullseye patterns cannot be created beyond the point of futility. Below it, they can establish a leakproof area larger than a single FOV. The certainty provided by the bullseye comes at the expense of speed: conventional search patterns can cover the same area more quickly. This may be a valuable trade in searches on high priority objects.

1. INTRODUCTION

Space Domain Awareness (SDA) involves detecting, tracking, identifying, and cataloging some 27,000 known satellites or pieces of debris, a number which is only growing [1]. Maintaining each object in the catalogue requires tasking a sensor to look for it at its predicted position, taking a measurement, and updating the existing state and uncertainty estimate to account for this new observation. Sensor time is very valuable due to the limited number of SDA sensors. Resources must be tasked efficiently to maintain high quality catalogue estimates.

For well-behaved, predictable objects, occasional observations are sufficient to maintain custody. High priority, highly maneuverable, or unpredictably perturbed RSOs (such as HAMRs or asteroids) may require frequent revisits, however. It is possible that some objects won't be where they are expected, or that their covariance covers a larger region of space than the field of view (FOV) of the sensor. In this case, a search pattern may need to be implemented. A search pattern covers some defined area or volume of space by moving the boresight and FOV of the sensor, with the aim of observing known (or finding previously unknown) objects [2, 3]. Throughout this paper, a *dwell* is used to refer to the sensor's FOV while it is making an observation.

The majority of search patterns are designed to do either general search or specific object detection. A general search pattern covers some region of space in a defined amount of time, monitoring the states of RSOs in the region. In a specific search pattern, successive dwells of the sensor are arranged to cover an object's uncertainty area when it is too large to fit within one FOV. There is an inherent trade between better sensitivity (for optical sensors) or decreased range ambiguity (for radar sensors) and scan speed. Scanning faster increases the chance of at least one detection, but decreases the sensitivity (optical) or range unambiguity (radar). Ideally, the scan speed is chosen to optimize this trade, and successive dwells are tiled such that there are no "gaps" between them. Examples of conventional search patterns include rasters and fences.

Even without gaps, a search pattern is not guaranteed to have a chance at detecting the RSO, which could potentially move from an unsearched area into a previously searched area, potentially being missed by the scan. This could create a harmful scenario where sensor operators believe they have confirmed that the object was not within the

* Corresponding Author: Daniel.J.Mulligan@saic.com

searched area when, in fact, it was. *Leakproof* search patterns prevent such scenarios. A search pattern is leakproof if the RSO is kinematically guaranteed to be detected if it is within some area when the search begins. The leakproof area is generally smaller than the total area covered by the search. For high priority objects, especially those with poor position estimates or irregular maneuvers, leakproof searches will either observe the RSO or exclude the searched region with certainty.

In the literature and in this paper, leakproof is assumed to encompass kinematics only. That is, given bounds on the RSO's maneuverability, as well as constraints on the SDA sensor's slew and dwell times, the RSO is guaranteed to be within at least one of the sensor's dwells. We do not consider the probability of detection within a particular dwell. This is tantamount to assuming that the sensor is well-designed, and has sufficient sensitivity for detecting objects at the expected range and rate of the RSO. It is therefore critical to apply any scan time constraints imposed by sensitivity or range unambiguity requirements.

At least one other leakproof pattern, the "bowtie", does exist [4]. It is a fence-type pattern that will detect objects as they cross it, provided the heading of the RSO is known within some uncertainty. It is particularly well-suited to the low-earth orbital (LEO) regime. Spiral or other circular search patterns are occasionally seen in the literature [3], but to the best of our knowledge, there has been no attempt to determine if they are leakproof, or provide a precise method for determining the actual sensor boresight vectors that comprise the pattern. For the special case of searching the entire geostationary (GEO) belt visible from the sensor's location on the ground, a leakproof search strategy is presented in [5].

In this paper, we present a novel, sensor-agnostic search pattern, the "bullseye", which consists of concentric rings of discrete dwells. It guarantees leakproof detection of an RSO moving in any direction with angular speed less than some assumed maximum in the sensor's frame, provided it is within a particular angular radius when the search begins. In Section 2, we provide an overview of the bullseye and introduce the notation used throughout the rest of this paper. In Section 3, we make kinematic arguments to arrive at the leakproof constraints, and parameterize the solution space. In Section 4, we provide our method for finding a solution that satisfies constraints, and explicitly show one method for determining the sequence of sensor boresight vectors comprising the solution. Section 5 presents numerical results from applying our solution method to a realistic SDA scenario. We first show results from a Monte Carlo simulation validating that the pattern is indeed leakproof. Then, we highlight the challenges encountered in finding optimal solutions and illustrate how the solution changes with different choices for parameters and optimization strategies. Section 6 concludes this work, discussing the contexts in which conventional scan patterns may not be adequate and implementation of the bullseye would be beneficial.

2. BULLSEYE DESCRIPTION AND NOTATION

The bullseye search pattern is comprised of concentric rings of dwells, as illustrated in Fig. 1. The dwell FOV is defined by cone angle Ψ. The sensor remains at each dwell for an integration time τ, and moves between dwells according to its movement capabilities. An electronically steered radar array may need virtually no movement time, whereas an optical telescope may take longer to slew and settle between dwells. We abstract these details into the term $t_s(\beta)$ – the time for the sensor to slew through an angle β between dwells.

The center of the first dwell in the middle of the bullseye is marked by the point $\mathcal{O}$, which lies on a unit sphere with the sensor at its center. The radius of each ring is measured from $\mathcal{O}$ to the centers of the ring's dwells, and is denoted R_n for ring n. This is illustrated in Fig. 2. The RSO of interest is assumed to have a predicted position and velocity at the beginning of the search, along with associated uncertainties. The state of the RSO is

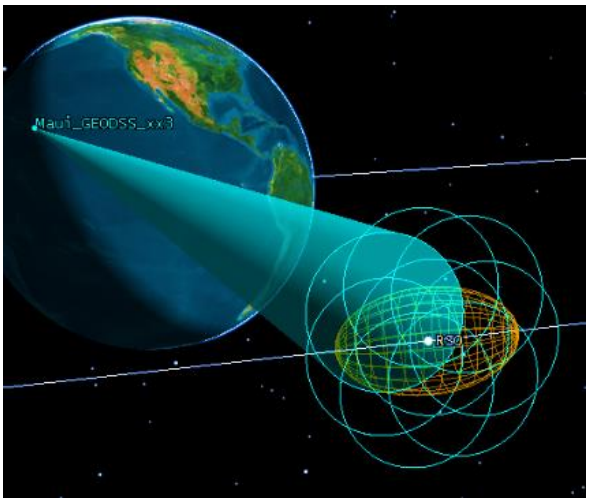

Fig. 1. The Maui_GEODSS_xx3 sensor has just completed the central dwell and first ring of dwells of a bullseye search pattern. The search is centered on the predicted position of the RSO, with uncertainty ellipsoid shown in orange.

projected into the spherical coordinate system centered on the sensor, since we are only interested in whether the RSO is within the sensor's FOV. The scan is also constructed in this coordinate system. While not strictly required, typically the point $\mathcal{O}$ would coincide with the predicted position of the RSO at the start of the search. We define $\omega_{\max}$ to be the maximum angular speed of the RSO in the sensor's reference frame. It is assumed to include the velocity uncertainty, such that it is truly the maximum possible speed of the RSO.

For convenience, the notation used throughout the rest of the paper is defined in Table 1. A few derived quantities which will be useful in later sections are also defined.

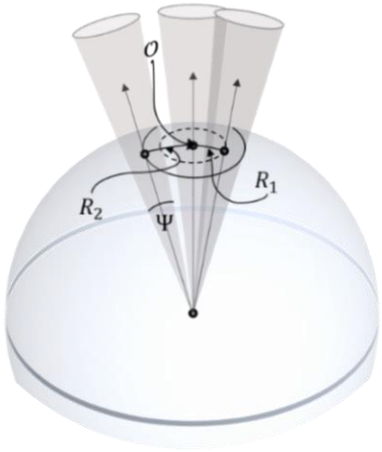

Fig. 2. Diagram illustrating the basic geometry of a bullseye pattern. Dwells in the first ring have boresights that lie on the dashed circle, and dwells in the second ring lie on the solid circle. Two representative dwells are shown, in addition to the central dwell. Subsequent rings are omitted for clarity.

Table 1. Bullseye pattern notation conventions.

Symbol	Description	Calculation
Ψ	Angular size of sensor FOV	-
$\mathcal{O}$	Bullseye's central boresight on unit sphere	-
R_n	Angular radius of the n^{th} ring	-
J_n	Number of dwells in the n^{th} ring	-
τ	Integration time of a dwell	-
$t_s(\beta)$	Time for sensor to slew an angle β between dwells	-
T_n	Total time for sensor to complete ring n	$= J_n\tau + \sum_{j=1}^{J_n} t_s(\beta_j)$
$\omega_{\max}$	Maximum expected angular speed of RSO in sensor's frame	-
δ_{dw}	Angular distance RSO can travel between successive dwells	$= \omega_{\max} t_s(\beta_{j,j+1})$
δ_n	Angular distance RSO can travel in time to complete ring n	$= \omega_{\max} T_n$

3. LEAKPROOF CONSTRAINTS

Each bullseye search is designed for a particular RSO, and establishes a certain leakproof area. If the RSO resides within this area at the beginning of the search, it is kinematically guaranteed to be detected by the time the search finishes. A single dwell is therefore leakproof, since if the RSO is in the FOV during a dwell, it will be detected. An area larger than a single FOV can be made leakproof by overlapping subsequent dwells with previously searched areas, to ensure that the RSO has not moved into that area since it was last scanned. The amount of overlap must be greater than the maximum possible distance the RSO could have moved in the time between dwells. This is the basic principle used to construct the bullseye search.

The bullseye begins with a single dwell, considered to be "Ring 0" of the bullseye. Each subsequent ring must enlarge the area of the search while maintaining leakproofness. To accomplish this, we first establish the leakproof area of a ring of dwells, which is shaped like an annulus. Any RSO within this annulus when the ring begins will be detected by the time it completes. By overlapping the ring's annulus with that of the previous ring in a particular way, the leakproof area of the search pattern can be enlarged.

An RSO with a velocity component in the pattern's azimuthal direction against the direction of the scan could potentially move from an unsearched area to a previously searched area, causing a leak. Referring to Fig. 3, consider an RSO which starts either at point D^- or D^+ at the end of the dwell centered on C_1. If the RSO is given sufficient time to reach point P^- or P^+ before the dwell centered on C_2 begins, it will not be seen by the second dwell. D^+ and D^- are thus chosen such that the shortest distance from the boundary of the first dwell to the boundary of the second exceeds the largest distance the RSO can move between dwells – that is, $\overline{DP}^{\pm} \geq \delta_{dw}$. Inner and outer radii, r_n^- and

r_n^+, are defined at the saturation of these bounds: $r_n^\pm = \widehat{\mathcal{O}D}^\pm$ such that $\widehat{DP}^\pm = \delta_{dw}$. We cannot make leakproof guarantees in the region outside of the inner and outer radii, and are only interested in the region between them. There, we will show that the ring is leakproof to azimuthally moving RSOs and that they are related to the radii of the ring's leakproof annulus.

An interesting case arises at the closure of the ring, between the first and last dwells. In Fig. 4, dwells proceed counterclockwise, beginning with the dwell labeled C_1 and ending with the dwell labeled C_{J_n}. Consider those RSOs on the trailing boundary of the first dwell. In the time T_n it takes to complete the ring, RSOs can cover an angular distance $\delta_n = \omega_{\max} T_n$. If the RSO can make it from the trailing edge of the first dwell to the leading edge of the last dwell by the time the ring completes, it may not be seen by any dwell. Thus, the overlap must be such that the distance between points $D_{J_n}^-$ and D_1^- is at least δ_n.

With the three conditions $\widehat{DP}^\pm \geq \delta_{dw}$ and $\widehat{D_{J_n}D_1}^- \geq \delta_n$, the region between the inner and outer radii of a ring is leakproof to RSOs moving in the pattern's azimuthal direction. We now turn to the radial direction, reminding the reader that "radial" here is really an angular distance denoting the great circle arc between a point and the point at the center of the bullseye. Consider RSOs that begin at the outer radius of the previous ring, and therefore may have been missed by the dwells of that ring. Those traveling radially inward may reach a distance of δ_n by the time the current ring completes. So, if the inner radius of the current ring is arranged to overlap the outer radius of the previous ring by at least δ_n, these RSOs will be seen by at least one dwell of the current ring. Similarly, radially-outward traveling RSOs will be seen as long as the difference between the outer radii of the current and previous ring is at least δ_n. This is illustrated in Fig. 5.

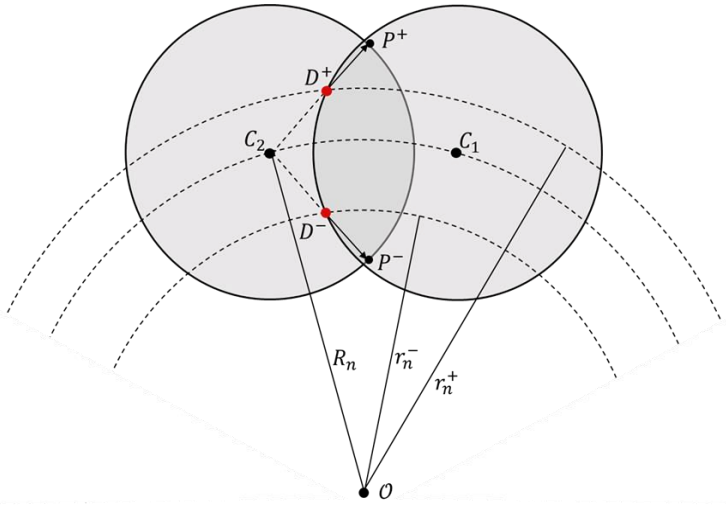

Fig. 3. Diagram showing the geometry of two adjacent dwells in ring n. The first and second dwells are shown, with centers at points C_1 and C_2, respectively. Both centers lie along the circle of radius R_n centered on $\mathcal{O}$ at the center of the bullseye pattern. RSOs located at D^- and D^+ at the end of the first dwell travel to points P^- and P^+, respectively, before the second dwell begins. The inner and outer radii are defined as $\widehat{\mathcal{O}D}^- = r_n^-$ and $\widehat{\mathcal{O}D}^+ = r_n^+$, respectively.

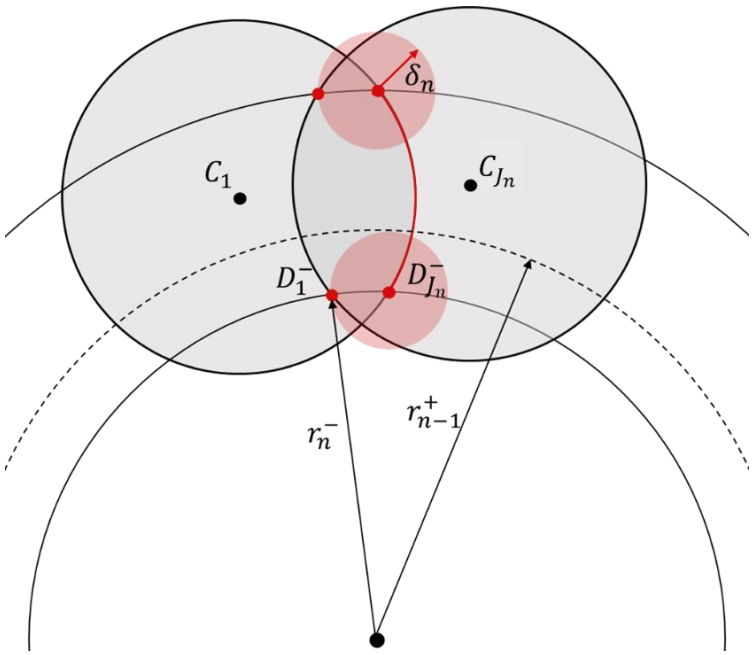

Fig. 4. Diagram showing the required overlap between the first and final dwells of a ring, with centers at C_1 and C_{J_n}, respectively. Successive dwells proceed in the counterclockwise direction. To avoid missing RSOs on the trailing edge of the first dwell between the inner and outer radii, and traveling counterclockwise, the shortest distance between points $D_{J_n}^-$ and D_1^- must be at least the distance the RSO can travel during the ring, δ_n.

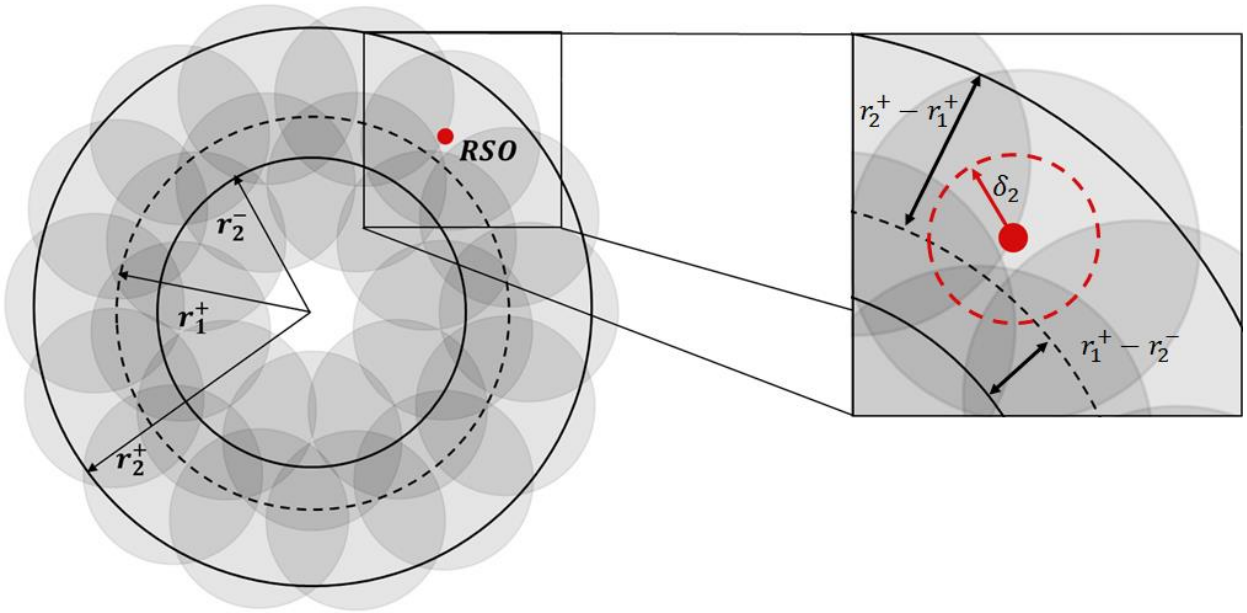

Fig. 5. Diagram showing the required overlap between successive rings in a bullseye. At the beginning of the second ring, any RSO that starts on r_1^+ and travels radially inward will be seen by a dwell in the second ring, provided $r_1^+ - r_2^- \geq \delta_2$. Similarly, those traveling radially outward from r_1^+ will be seen by the second ring if $r_2^+ - r_1^+ \geq \delta_2$.

If, at the beginning of ring *n*, the RSO started at a radius r such that $r_n^- \leq r < \delta_n + r_n^-$, it would have already been seen by the previous ring. If it started at radius r such that $0 \leq r_n^+ - r < \delta_n$, it may not be seen by the current ring, but it will be seen by the next ring. Of course, if the current ring is to be the last one, we can't rely on the next ring. But, we will define the leakproof area of the complete scan such that it does not include this region.

There are thus five leakproof constraints:

$$r_n^- = \widehat{OD}^- \quad s.t. \quad \widehat{DP}^- \geq \delta_{dw}, \tag{1}$$

$$r_n^+ = \widehat{OD}^+ \quad s.t. \quad \widehat{DP}^+ \geq \delta_{dw}, \tag{2}$$

$$r_{n-1}^+ - r_n^- \geq \delta_n, \tag{3}$$

$$r_n^+ - r_{n-1}^+ \geq \delta_n, \text{ and} \tag{4}$$

$$\widehat{D_{J_n}^- D_1^-} \geq \delta_n. \tag{5}$$

Note that various time components are implicit in the leakproof constraints. For instance, δ_{dw} depends on the time between successive dwells, and δ_n depends on the integration time, the time between dwells, and the number of dwells in a ring. A bullseye that satisfies these constraints will create a leakproof area such that any RSO beginning within the area will be detected before the search ends. The area is defined in terms of the leakproof radius, R_{LP}. Given a total scan time ΔT, the largest angular distance the RSO can cover is $\omega_{\max}\Delta T$. If N rings comprise the bullseye, the leakproof radius is illustrated in Fig. 6 and is given by

$$R_{LP} = r_N^+ - \omega_{\max}\Delta T. \tag{6}$$

Ideally, we would like to know how to find solutions satisfying the leakproof constraints that are "optimal" in some way. In addition to the location of the central dwell, a solution requires specifying the total number of rings, and for each ring, the radius, number of dwells, and angle of each dwell. That is, it is the set $\{R_n, \theta_k \mid k = 1, \ldots, J_n\,; n = 1, \ldots, N\}$ where each radius and angle are measured relative to the central dwell. Changes in the leakproof radius with

variations between solutions are of primary interest to SDA applications. We may wish, for instance, to find the solution that maximizes the leakproof radius. Or, we may want to minimize the total search time while meeting some minimum leakproof area. Analytically, this is an extremely complicated problem that is often counterintuitive, because of non-trivial couplings of the constraints to the problem's time scales. For example, we may expect that a ring with a large outer radius would yield a large leakproof radius. But, because this ring would require more dwells and more time to complete, the RSO can travel further before the search completes, and the leakproof radius would be smaller. Furthermore, solutions inherently depend on the sensor's slew capabilities, through $t_s(\beta)$.

The problem is thus best approached numerically. This allows the bullseye designer to use any appropriate model for the sensor's slew capabilities, and allows for R_{LP} to be optimized in the way that best suits the SDA mission. In the next two sections, we provide our numerical approach to finding a solution, and present results for a typical SDA scenario. We also comment on how the results change under changes to the bullseye design parameters.

4. BULLSEYE IMPLEMENTATION

The parameter space containing bullseye patterns that satisfy the leakproof constraints is large and underdetermined. In order to reduce it, we first assume that dwell centers are evenly spaced in angle from the center $\mathcal{O}$, as shown in Fig. 7. In this case, solutions can be defined by four parameters: the number of rings N, the radius of each ring R_n, the number of dwells in each ring J_n, and the angle of the final dwell θ_{J_n}, which is a free parameter not restricted to be less than 2π.

Next, we assume that the last dwell of a ring is coincident with the first

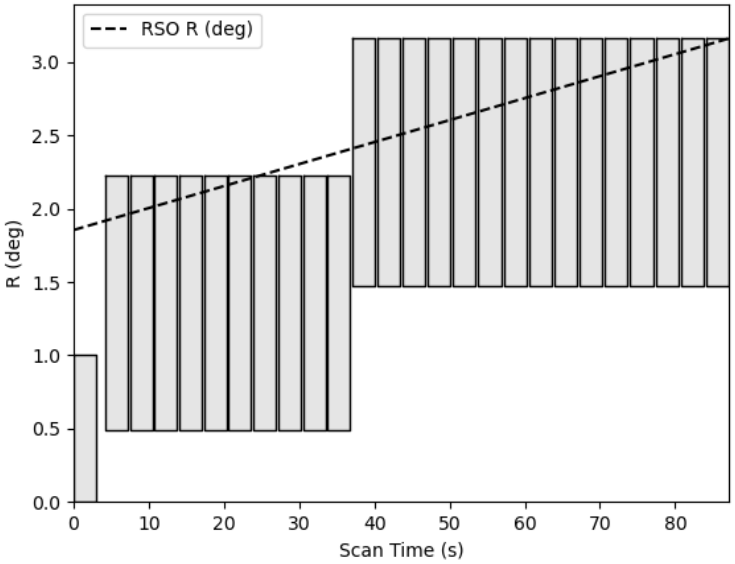

Fig. 6. Diagram showing a bullseye's leakproof radius. Each gray bar is a dwell, extending from each ring's inner radius to its outer radius. The bar's thickness indicates the time required for one dwell, and bars are separated by the time required to travel between dwells, which was quite short in this particular scenario. The dashed line indicates an RSO traveling radially outward at its maximum angular rate, so that $R = R_{LP} + \omega_{max} t$ (converting from radians to degrees as appropriate). The last dwell *just* catches this RSO. So, R_{LP} is the intersection of the dashed line with the vertical axis. Since each ring is also designed to be leakproof to azimuthal motion, any RSO beginning the scan with $R \leq R_{LP}$ will be seen by the time the last ring completes.

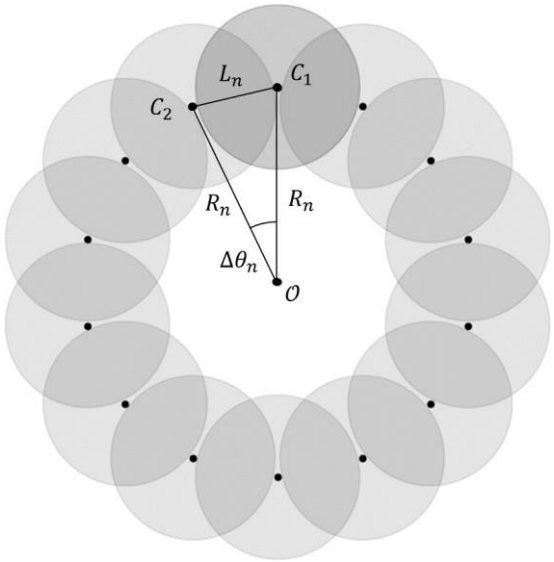

Fig. 7. Diagram showing the arrangement of dwells within a ring in our specific implementation: the dwells are spaced evenly by $\Delta\theta_n$, and the last dwell centered on C_{J_n} is coincident with the first dwell C_1.

dwell – that is, $\theta_{J_n} = 2\pi$. This is usually sufficient to satisfy the fifth constraint. It becomes insufficient as the dwell spacing shrinks: as $\Delta\theta_n \to 0$, the inner and outer radius $r_n^{\pm} \to R_n \pm \Psi$, making $\widehat{D_J^- D_1^-}$ small. Furthermore, small $\Delta\theta_n$ require a large number of dwells, so δ_n becomes large, and constraint 5 may fail. However, large numbers of dwells require long search times, and since the leakproof radius decreases with total search time, we are not interested in these potential solutions.

For the remaining parameters $\{R_n, J_n | n = 1, \dots, N\}$, a Python tool was developed to find solutions that meet the leakproof constraints. By convention, the center dwell is $n = 0$ with $R_0 = 0$. For each ring, $\theta_{1,n} = 0$, and 500 values of R_n together with 300 values of J_n are tested, for a total of 150,000 possible combinations. Of those combinations that meet all of the leakproof constraints, the one that yields the largest leakproof radius is chosen, provided this radius is larger than the leakproof radius found with the previous ring. The search is terminated when no possible combination meets the leakproof constraints, or when all solutions yield a smaller leakproof radius than the one already found.

The two-dimensional diagrams of this section and the preceding section can be misleading. We remind the reader that straight lines in these figures are actually great-circle arcs on the surface of a unit sphere centered on the sensor (see Fig. 2). To avoid any confusion, we explicitly explain the calculations. Assume we are interested in searching for a particular RSO. We will position the first dwell to coincide with the predicted position of the RSO at the start of the search, and design the bullseye for a particular $\omega_{\max}$, which should include any uncertainty coming from poor state estimates, potential maneuvers, and so on. Accurate estimation of this rate is important. If it is too small, the bullseye will not be leakproof to the true RSO. If it is too large, the bullseye solution will cover a smaller area than it could with a better estimation.

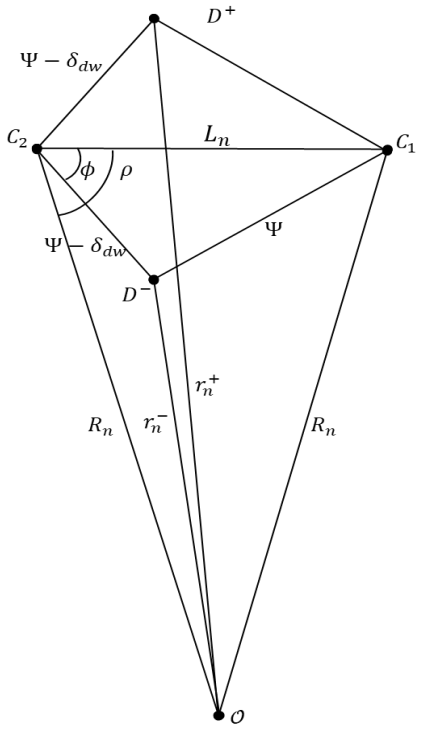

Fig. 8. Geometry for determining the inner and outer radii of a ring.

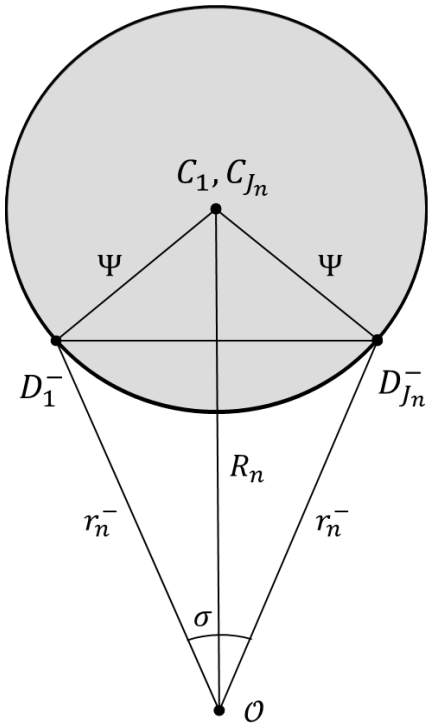

Fig. 9. Geometry for calculating $\widehat{D_{J_n}^- D_1^-}$, in order to check that the constraint in Eq. 5 is satisfied.

After positioning the center dwell, we then proceed to design each ring in succession. Each choice of (R_n, J_n) defines the spacing between dwells for that ring:

$$\Delta\theta_n = \frac{2\pi}{J_n - 1}.$$

The arc length, L_n in Fig. 7, can be calculated with the aid of the spherical law of cosines (SLOC),

$$L_n = \cos^{-1}(\cos^2 R_n + \sin^2 R_n \cos \Delta\theta_n).$$

Given a model for the sensor's slewing capabilities, the time to slew between dwells is then determined by $t_s(L_n)$. The time for a ring is then completely determined, it includes the slew time from the last dwell of the previous ring to the first dwell of the current ring, and is given by

$$T_n = t_s(R_n - R_{n-1}) + (J_n - 1) \cdot t_s(L_n) + J_n \cdot \tau.$$

We ensure the first two constraints (Eqs. 1-2) are satisfied by setting the inner and outer radii to the saturation of the bounds. The SLOC is again applied numerous times to calculate the inner and outer radii. Angles and arcs are defined as in Fig. 8. Geometry gives

$$\phi = \cos^{-1}\left(\frac{\cos\Psi - \cos(\Psi - \delta_{dw})\cos L_n}{\sin(\Psi - \delta_{dw})\sin L_n}\right),$$

$$\rho = \cos^{-1}\left(\frac{1 - \cos L_n}{\tan R_n \sin L_n}\right),$$

$$r_n^{\pm} = \cos^{-1}(\cos R_n \cos(\Psi - \delta_{dw}) + \sin R_n \sin(\Psi - \delta_{dw}) \cos(\rho \pm \phi)).$$

Constraint 5 can be checked by calculating the arc length $\widehat{D_{J_n}^- D_1^-}$. This is quite straightforward, since the first and last dwell coincide. Any combination (R_n, J_n) that does not satisfy the constraint is not leakproof, and excluded from the solution set. The geometry is shown in Fig. 9.

$$\sigma = 2\cos^{-1}\left(\frac{\cos\Psi - \cos R_n \cos r_n^-}{\sin R_n \sin r_n^-}\right), \text{and}$$

$$\widehat{D_1^- D_{J_n}^-} = \cos^{-1}(\cos^2 r_n^- + \sin^2 r_n^- \cos\sigma).$$

The combinations (R_n, J_n) that survive after checking the fifth constraint are arranged such that the overlap between the inner radius and the outer radius of the previous ring satisfy the third constraint. That is, the condition $r_{n-1}^+ - r_n^- = \delta_n$ is enforced. The fourth constraint is then checked, so that any solutions with $r_n^+ - r_{n-1}^+ < \delta_n$ are excluded. We are left with a set of solutions that satisfy all of the leakproof constraints. Assuming the scan would end with this ring, the leakproof radius is $R_{LP,n}$, calculated from Eq. 6. The ring solution which yields the largest $R_{LP,n}$ is chosen, provided $R_{LP,n} > R_{LP,n-1}$. If this cannot be satisfied, or there are no solutions, then no more rings can be created.

The only task remaining is to translate each ring's solution (R_n, J_n) into a boresight vector telling the sensor where to point, most conveniently written as a sequence of azimuth and elevation coordinates (α, ε) relative to the sensor. With θ_j denoting the angle of the j^{th} dwell in the ring, as in Fig. 7, and (α_0, ϵ_0) denoting the azimuth and elevation of the bullseye's central dwell,

$$\varepsilon = \sin^{-1}(\sin\varepsilon_0 \cos R_n + \cos\varepsilon_0 \sin R_n \cos\theta_j)$$

$$\alpha = \alpha_0 + \tan^{-1}\left(\frac{\sin\theta_j \sin R_n \cos\varepsilon_0}{\cos R_n - \sin\varepsilon_0 \sin\varepsilon}\right).$$

In the next section, we show an example of our implementation with parameters representative of a realistic SDA mission, and describe results from a Monte Carlo simulation validating the leakproof nature of the pattern. We also comment on how the solution changes with different optimization strategies, and with different sensor parameters.

5. RESULTS & DISCUSSION

Two python tools were developed to design and evaluate bullseye search patterns. The first numerically constructs solutions to the leakproof constraints as described in the implementation section above. The second validates the leakproof constraints in a Monte Carlo-type (MC) simulation. 10,000 points are randomly distributed inside the bullseye's leakproof radius, each representing a possible state of the RSO of interest. When the search

begins, they immediately start traveling along randomly oriented great circle arcs at the maximum RSO angular rate for which the pattern was designed. As the search proceeds, a point is counted as detected if it is inside the sensor's FOV during a dwell. Note that the percentage of points detected is *not* the same as the probability of detection, since the points are drawn from a uniform distribution rather than a probability distribution constructed from the state covariance of the RSO. The MC simulation only allows us to say whether or not a pattern is leakproof. It has not yet revealed a leak in any of the scenarios we have tested, further validating the arguments leading to the leakproof constraints.

We created a realistic, representative example to illustrate a scenario in which a bullseye scan could be used. Consider an RSO in a GEO orbit inclined at 15°. Such an object has a maximum angular rate of about 3.5 arcsec/s relative to a point on the earth's surface [6]. We use this value as a reasonable $\omega_{\max}$. The SDA sensor is assumed to be a telescope with a circular FOV of 0.5° diameter, and we use an integration time of 3 seconds. Longer integration times may be needed, depending on the requisite sensitivity – we will comment on this at the end of this section. The telescope is assumed to take 5 seconds total to move between dwells, including any necessary settle time.

The bullseye pattern created by maximizing the leakproof radius of each ring consists of 5 rings for a total of 69 dwells, taking 547 seconds to execute. The resulting leakproof area has a diameter of 1.53°. The dwell pattern is illustrated in Fig. 10, with the solid black circle indicating the leakproof radius. The area of a circle of radius ρ on the surface of a unit sphere is $A = 2\pi(1 - \cos\rho)$, so the leakproof area of the bullseye is 9.33 times larger than that covered by a single FOV.

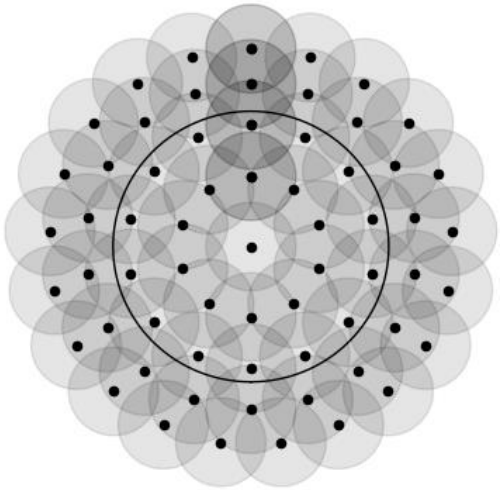

Fig. 10. Notional bullseye scan showing the central dwell and 4 rings designed to capture the RSO in the scenario described in Section 5. The solid circle indicates the leakproof radius, and has a diameter of 1.53°.

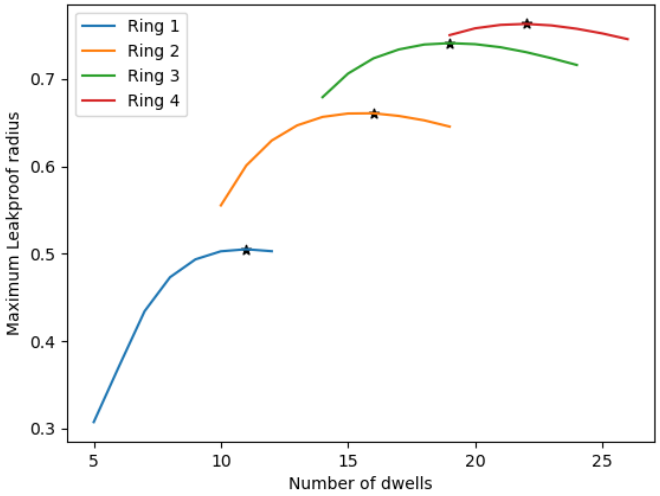

Fig. 11. For each discrete number of dwells J_n, the ring radius R_n that yields the largest leakproof radius is chosen. This maximum leakproof radius is shown as a function of J_n for each ring. The black stars indicate the chosen solution (R_n, J_n) for each ring.

The strategy of choosing the combination (R_n, J_n) yielding the maximum leakproof radius for each ring does not necessarily yield the largest leakproof radius for the overall pattern. For the bullseye illustrated above, Fig. 11 shows each ring's leakproof radius as a function of the number of dwells in the ring. For each J_n, there are multiple R_n that may meet the leakproof constraints. So, the curves in Fig. 11 are created by choosing the R_n that yields the *maximum* leakproof radius for each J_n. The black star on each curve marks the chosen solution. Note, however, that each ring's leakproof radius depends on the choice of solution for all the previous rings, since R_{LP} depends on the total time up to the current ring. Choosing a different solution e.g. for Ring 1 changes the curves for Rings 2-4.

Table 2 shows the effect on the bullseye's leakproof radius if different J_1 are chosen for the first ring. Assuming we still choose the J_n yielding the ring's maximum leakproof radius for rings 2-4, choosing $J_1 = 11$ gives

the maximum leakproof radius for the first ring, $R_{LP,1}$, while choosing $J_1 = 9$ gives the maximum *overall* leakproof radius, $R_{LP,4}$. This is somewhat intuitive: performing fewer dwells in the first ring saves time, allowing the scan to move more quickly to the next ring. In Fig. 11, the curvature near the maximum of each ring is small, and there
appears to be an inflection point, markedly in the early rings. Beyond the inflection point, the scan time grows with each dwell added, but the ring's leakproof radius is only marginally improved. The overall leakproof radius shrinks with increasing scan time. If such an inflection point exists for a ring, this suggests a better strategy for maximizing R_{LP} than the approach we employed in Section 4. We intend to explore this further in future work.

The bullseye is not a useful search strategy for every situation. For instance, if the RSO's $\omega_{\max}$ is too large compared to the sensor's capabilities, the "bullseye" might at worst consist only of the single central dwell – rings cannot be created without violating the leakproof constraints. This might occur, for instance, if integration times need to be long to achieve a requisite sensitivity, or if the time to move and settle between dwells is long. Of course, if $\omega_{\max} > \Psi/\tau$, the RSO could potentially be moving too fast for even a single dwell to capture it. This would indicate that τ needs to be shorter, or that a bullseye is simply infeasible in this scenario.

Table 2. Variation in leakproof radius at the end of rings 1 and 4, with different numbers of dwells chosen for ring 1.

J_1	$R_{LP,1}$	$R_{LP,4}$
5	0.307°	0.741°
6	0.372°	0.749°
7	0.434°	0.763°
8	0.473°	0.770°
9	0.494°	0.771°
10	0.503°	0.770°
11	0.505°	0.763°
12	0.503°	0.757°

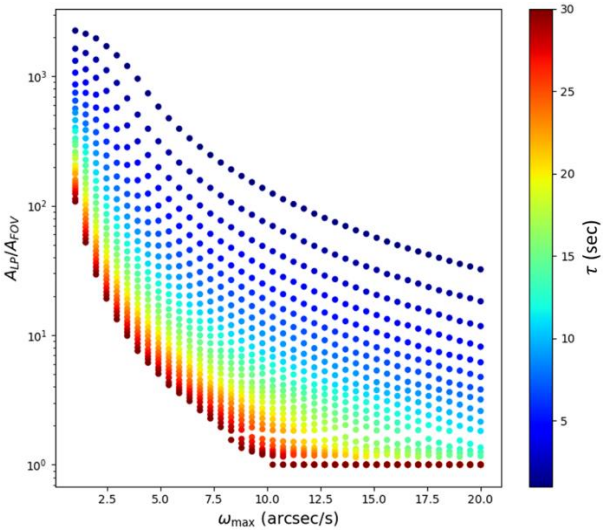

Fig. 12. For each choice of RSO angular speed on the horizontal axis, each point represents a bullseye solution, with color indicating the integration time at each dwell. The vertical axis shows the ratio of the bullseye's leakproof area to that of a single dwell. The FOV and slew time were held fixed at 2° diameter and 2 seconds, respectively.

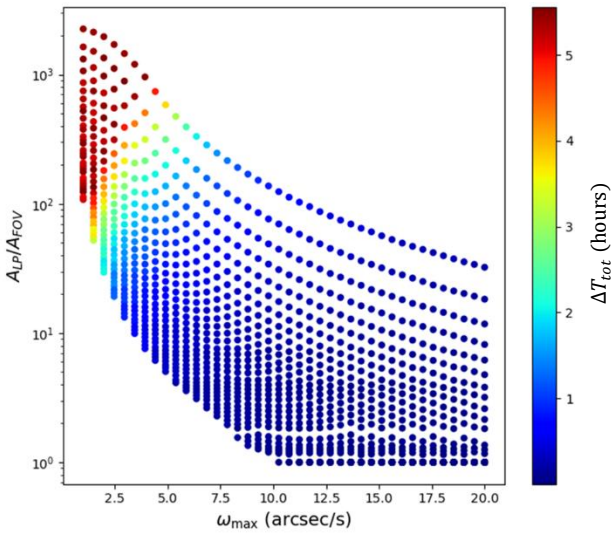

Fig. 13. The same data as in Fig. 12 is shown, except the color axis represents the total time for the scan, in hours. Note here that very long scan times occur when the RSO's ω_{max} is small, almost independently of integration time, because the small ω_{max} allows each ring to take more time and still meet Eqs. 3 and 4.

Figs. 12 and 13 help to assess the range of scenarios in which a bullseye is both feasible and useful. Each point on the scatter plots represents a solution found through the method described in Section 4. The FOV and time

between dwells were fixed, at 2° diameter and 2 seconds, respectively. In both figures, the horizontal axis is the RSO's $\omega_{\max}$, and the vertical axis is the ratio of the solution's leakproof area to that of a single dwell. In Fig. 12, the solutions are colored by the integration time of a single dwell. In Fig. 13, they are colored by the total time required to complete the search. Where the area ratio $A_{LP}/A_{FOV} = 1$, the bullseye consists of a single central dwell – no solutions can be found that further expand the leakproof area. This occurs as $\omega_{\max}$ increases, and also as the integration time increases at a fixed $\omega_{\max}$. Conversely, very large area ratios occur when $\omega_{\max}$ is small, so that increasingly larger rings with more dwells can be created. Notice that all of the solutions in the upper left of the figure with $A_{LP}/A_{FOV} > 100$ and $\omega_{\max} < 2.5$ arcsec/s take upwards of 5 hours to complete. In practical scenarios, these solutions should probably be truncated at fewer total rings, which would somewhat decrease the leakproof area, but dramatically decrease the required time. Searches must balance the leakproof coverage with the time required to complete them.

One final, interesting result is shown in Fig. 14. There, we have constructed bullseye solutions according to the method in Section 4, and have allowed all of the parameters to vary. The RSO's angular rate varied from $1 - 20$ arcsec/s, the integration time from $1 - 30$ s, slew time from $2 - 5$ s, and FOV beamwidth from $1 - 5°$, for a total of 7,200 parameter combinations. As in Figs. 12-13, the vertical axis shows the ratio of the leakproof area to that of a single FOV. On the horizontal axis is $\omega_{\max}(\tau + t_s)/\Psi$ – that is, the ratio of the angular distance the RSO can travel during the time to move to and complete a dwell to the size of the FOV. The variance of data in the upper left is an artifact due to placing an upper limit on R_n in the search for solutions, and the broken region in the vicinity of 0.04 on the horizontal axis is likely due to insufficient sampling resolution on R_n. Aside from these, solutions appear to lie on a curve. This provides a convenient "rule of thumb" for determining contexts in which the bullseye both is feasible and may provide a useful search strategy. If this criterion is satisfied, a bullseye that gives a larger leakproof area than a single dwell is generally possible. If it is not, the bullseye is a single central dwell, and other search strategies should be employed. We therefore call the saturation of the bound in Eq. 7 the "point of futility".

$$\frac{\omega_{\max}(\tau + t)}{\Psi} \lesssim 0.05 \rightarrow \frac{A_{LP}}{A_{FOV}} \gtrsim 1. \qquad 7$$

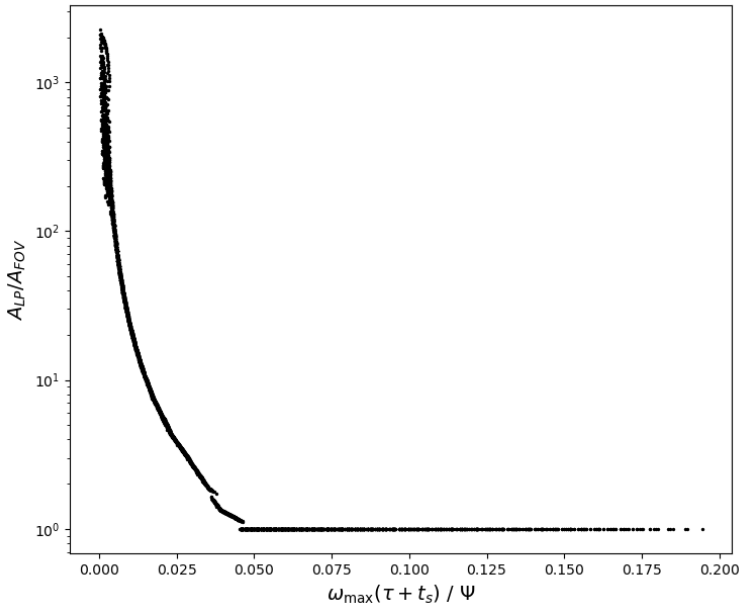

Fig. 14. A_{LP}/A_{FOV} is shown as a function of $\omega_{max}(\tau + t_s)/\Psi$ for 7,200 bullseye solutions. None of the parameters is held constant: ω_{max}, τ, t_s, and Ψ all vary to create 7,200 different combinations.

6. CONCLUSIONS

The bullseye is a new, sensor-agnostic, leakproof search strategy consisting of concentric rings of discrete dwells. The size of the leakproof area that can be searched depends primarily on $\omega_{\max}$, the maximum angular rate at which the RSO could potentially move, and also depends on the SDA sensor's slewing capability, required integration time, and FOV. In order to be leakproof, a bullseye solution must meet a set of constraints that are based on kinematic and geometric arguments. Constraints are written in terms of the RSO's maximum angular rate in the sensor's reference frame, the sensor's slew capability, integration (or dwell) time, and angular size of the FOV. Solutions are parameterized in terms of the number of rings, radius of each ring, number of dwells in each ring, and azimuthal position of each dwell relative to the center of the pattern. Due to the complex nature of the solution space and couplings between the constraints, solutions are best determined numerically. This is easily accomplished through the method detailed in Section 4.

Bullseye solutions have a characteristic leakproof radius, used to define a leakproof area in which any RSO moving slower than $\omega_{\max}$ is kinematically guaranteed an opportunity for detection. The size of the leakproof area grows as ω_{max} becomes smaller, as the dwell time and slew time between dwells shrinks, or as the size of a single dwell's FOV grows. However, expanding the leakproof area comes at the expense of disproportionately increased time to complete the scan. Given the integration time required to achieve the requisite sensitivity or range resolution, the time required to move between dwells, the angular size of the FOV, and the RSO's maximum angular speed, the "point of futility" defined by Eq. 7 demarcates parameter combinations for which useful bullseye solutions can be found. If leakproof guarantees are not required for a particular RSO, conventional scans can cover the same area much more quickly. The true value of the bullseye lies in its ability to either observe the RSO or exclude with certainty a particular region of space.

REFERENCES

[1] Garcia, M. (2021, May 26). "Space debris and human spacecraft," NASA. Retrieved August 11, 2022, from https://www.nasa.gov/mission_pages/station/news/orbital_debris.html

[2] S. Fedeler, M. Holzinger, W. Whitacre, " Optimality and Application of Tree Search Methods for POMDP-based Sensor Tasking," Proceedings of the AMOS Technical Conference, 2020.

[3] B. Quine, L Scott, C. Roberts, "Earthfence: a GEO capable deep space radar," Proceedings of the AMOS Technical Conference, 2020.

[4] D. Mattheison, "Bowtie Search Theory and Design," Radar 97 (Conf. Publ. No. 449), 1997, pp. 775-782.

[5] K. Poole, J. Woloschek, E. Murphy, J. Lefever, J. Breslin, "Strategies for Optimizing GEO Debris Search," Proceedings of the AMOS Technical Conference, 2006.

[6] L. Murphy, C. Gow, J. Lefever, D. Haeberle, J. Breslin, "Ground-Based Optical System Requirements for Performing a Non-Tasked and Leak-Proof Cataloging Mission at GEO," 2011.